

On asymmetry in Stewartson layers

G.J.F. Van HEIJST¹ and S.H. SMITH²

¹*Institute of Meteorology and Oceanography, University of Utrecht, Princetonplein 5, 3584 CC Utrecht, The Netherlands*

²*Department of Mathematics, University of Toronto, Toronto, M5S 1A1, Canada*

Received 9 May 1989; accepted 20 June 1989

Abstract. There are two basic conclusions reached in this paper. It is shown first that the structure of free shear layers in a rotating fluid change only slightly when an asymmetry is introduced into the geometry; in fact, once a Poisson equation which describes the flow in the interior Taylor column is solved, the behaviour in both $\frac{1}{2}$ and $\frac{1}{4}$ -layers is understood for all situations. The second result derived is that when the Stewartson layers are along solid sidewalls in an asymmetric configuration, then the velocity within the interior has additional components induced by the $\frac{1}{4}$ -layer; the first perturbation is $O(E^{\frac{1}{4}})$.

1. Introduction

The flow within axisymmetric Stewartson layers in a rotating fluid of low viscosity has been well understood for many years. Their structure was first presented by Stewartson [1], and a complete analysis of different possibilities for a variety of situations was given in the paper by Moore and Saffman [2]. The monograph by Greenspan [3] summarizes most of these early results, and also includes a discussion of differences when asymmetries are present. These comments (following the basic work of Hide [4]) are centred on the flow due to a distribution of sources and sinks on a circular cylinder, and it is shown that the essential features of the flow within the layers on the cylinder are unchanged whether there is axial symmetry or not – an asymmetric distribution affects just the radial velocity through an azimuthal pressure gradient. In fact, as Greenspan states, because the basic equations between the azimuthal and axial velocities do not involve the azimuthal co-ordinate, the boundary layer calculation for the circular cylinder applies as well to any vertical boundary of arbitrary cross section if the radial and azimuthal co-ordinates are replaced by co-ordinates in the normal and circumferential directions. The one solution which he presented for illustrative purposes was for an axisymmetric case.

Johnson [5] gives a full theoretical solution for one of the experiments conducted by Hide, where a line source and a line sink are placed symmetrically within a rotating finite circular cylinder. His main interest was in finding how the mass flux is transported through the different regions, which required an extensive analysis up to the third order in the interior; the Stewartson layers along the wall of the cylinder were described as part of the solution through solving Greenspan's equations.

The first intention of this paper is to extend these ideas through solving a specific problem – essentially the asymmetric split-disc problem – which gives rise to asymmetric free shear layers. A complete description can be given to the internal flow within the Taylor column, and also in both the Ekman and Stewartson layers surrounding it; in fact, the calculations for the particular case carry over for all situations once the slip velocity along the

boundary of the Taylor column are known. Effectively, we generalize the asymptotic approach of Moore and Saffman [2] in matching across different domains to gain a precise description of the dominant features of the flow, and thereby to strengthen our understanding of the effects of asymmetry. It is seen that the results from axisymmetric theory require only minimal changes.

However, if the geometry is changed so that the Stewartson layers are no longer free, but attached to a solid sidewall, there is an interesting difference. When the analysis is carried to higher orders in this situation it is found, in contrast to the axisymmetric problem with sidewalls, that the Stewartson layers play an active role in determining the higher-order geostrophic flow; the addition to the interior velocity is $O(E^{\frac{1}{2}})$. We can conclude that the development of this higher-order interior flow requires both the asymmetry and the attachment of the layer to a solid wall.

2. Basic problem

Fluid with density ρ and viscosity ν is constrained between two infinite discs represented by $z = 0, h$ which rotate with angular velocity Ω about the vertical z -axis to provide the basic solid-body rotation. A semi-circular portion of the lower disc, with radius a , rotates at a slightly different angular velocity $\Omega(1 + \varepsilon)$, where ε is the small Rossby number. Practically, the lower disc can be seen as having two sections, a main part which has a semi-circular hole, and a secondary part which can slide smoothly beneath the main part without any leaking of fluid. We introduce a cylindrical co-ordinate system (r, θ, z) in a frame of reference which rotates with angular velocity Ω , and in this frame write the radial, azimuthal and axial velocities as $\varepsilon\Omega au$, $\varepsilon\Omega av$ and $\varepsilon\Omega aw$ respectively. When, further, the pressure is defined by $\varepsilon\rho\Omega^2 a^2 p$, the equations of motion are

$$u_r + r^{-1}u + r^{-1}v_\theta + w_z = 0, \quad (2.1)$$

$$-2v = -p_r + E(u_{rr} + r^{-1}u_r - r^{-2}u + r^{-2}u_{\theta\theta} + u_{zz} - 2r^{-2}v_\theta), \quad (2.2)$$

$$2u = -r^{-1}p_\theta + E(v_{rr} + r^{-1}v_r - r^{-2}v + r^{-2}v_{\theta\theta} + v_{zz} + 2r^{-2}u_\theta), \quad (2.3)$$

$$0 = -p_z + E(w_{rr} + r^{-1}w_r + r^{-2}w_{\theta\theta} + w_{zz}); \quad (2.4)$$

E is the Ekman number for the flow, with $E = \nu/\Omega a^2$, which is to be taken as small throughout this study.

The boundary conditions for the problem as posed require

$$u = v = w = 0 \quad \text{on } z = 0, h, \text{ except}$$

$$v = r \quad \text{on } z = 0 \quad \text{for } r < 1 \text{ and } |\theta| < \frac{1}{2}\pi. \quad (2.5)$$

Because of the constraints of the Taylor–Proudman theorem, it is clear that it is only within the domain $r \leq 1$, $|\theta| \leq \frac{1}{2}\pi$, including the boundaries, that there are non-zero values for the velocities u , v , w , and so we can restrict the investigation to this domain from now on.

We first consider the flow in the Ekman layers. For the layer on the lower disc we write

$z = E^{\frac{1}{2}}\zeta$, and it follows for $\zeta = O(1)$, with slight adjustments to previous calculations (cf. Jacobs [6]), that

$$2u = -r^{-1}\mathcal{P}_\theta(1 - e^{-\zeta} \cos \zeta) + (2r - \mathcal{P}_r) e^{-\zeta} \sin \zeta, \quad (2.6)$$

$$2v = -r^{-1}\mathcal{P}_\theta e^{-\zeta} \sin \zeta + (2r - \mathcal{P}_r) e^{-\zeta} \cos \zeta + \mathcal{P}_r, \quad (2.7)$$

$$4w = -E^{\frac{1}{2}}\{1 - e^{-\zeta}(\cos \zeta + \sin \zeta)\}(4 - \nabla^2\mathcal{P}); \quad (2.8)$$

$\mathcal{P}(r, \theta)$ is the (still unknown) pressure in the interior of the fluid. For the Ekman layer on the upper disc we write $h - z = E^{\frac{1}{2}}\xi$, and see by similar arguments that

$$2u = -r^{-1}\mathcal{P}_\theta(1 - e^{-\xi} \cos \xi) - \mathcal{P}_r e^{-\xi} \sin \xi, \quad (2.9)$$

$$2v = -r^{-1}\mathcal{P}_\theta e^{-\xi} \sin \xi + \mathcal{P}_r(1 - e^{-\xi} \cos \xi), \quad (2.10)$$

$$4w = -E^{\frac{1}{2}}\{1 - e^{-\xi}(\cos \xi + \sin \xi)\}\nabla^2\mathcal{P}. \quad (2.11)$$

Consequently, for continuity of the axial velocity within the interior, it is necessary from (2.8) and (2.11) that

$$\nabla^2\mathcal{P} = 2.$$

If we write $u = \mathcal{U}(r, \theta)$, $v = \mathcal{V}(r, \theta)$ in the interior, it then follows that the stream function $\Psi(r, \theta)$, defined by $\mathcal{U} = r^{-1}\Psi_\theta$, $\mathcal{V} = -\Psi_r$, satisfies

$$\nabla^2\Psi = -1, \quad \text{plus } \Psi = 0 \text{ on the boundary,} \quad (2.12)$$

with $\mathcal{P} = -2\Psi + \text{constant}$. Finally, the axial velocity \mathcal{W} between the two Ekman layers is constant and equal to $-\frac{1}{2}E^{\frac{1}{2}}$; the total mass flux through the column is $-\frac{1}{4}\pi E^{\frac{1}{2}}$.

For the interior flow we write

$$\Psi(r, \theta) = -\frac{1}{4}r^2(1 + \cos 2\theta) + \Phi(r, \theta) \quad (2.13)$$

where Φ is harmonic for $r \leq 1$, $|\theta| \leq \frac{1}{2}\pi$ with $\Phi = 0$ on $\theta = \pm\frac{1}{2}\pi$ and $\Phi = \frac{1}{4}(1 + \cos 2\theta)$ on $r = 1$; the first term of (2.13) gives the particular integral of (2.12), and the second term is the harmonic term which ensures that Φ is zero on the rays $\theta = \pm\frac{1}{2}\pi$. It is now possible to write $\Phi = \sum_{n=0}^{\infty} a_n r^{2n+1} \cos(2n+1)\theta$, where $\cos(2n+1)\theta$ are the appropriate eigenfunctions, and the coefficients a_n must satisfy $\sum_{n=0}^{\infty} \cos(2n+1)\theta = \frac{1}{4}(1 + \cos 2\theta)$ for $|\theta| \leq \frac{1}{2}\pi$, from which it is found that $a_n = -4(-1)^n \pi^{-1} (2n-1)^{-1} (2n+1)^{-1} (2n+3)^{-1}$. The infinite series $\sum_{n=0}^{\infty} a_n r^{2n+1}$ can be summed through standard methods, and on taking real parts there follows

$$\begin{aligned} \Psi(r, \theta) = & -\frac{1}{4}r^2(1 + \cos 2\theta) + \frac{1}{2\pi} \left(r - \frac{1}{r}\right) \cos \theta \\ & + \frac{1}{4\pi} \left\{ \left(r^2 + \frac{1}{r^2}\right) \cos 2\theta + 2 \right\} \arctan\left(\frac{2r \cos \theta}{1 - r^2}\right) \\ & - \frac{1}{8\pi} \left(r^2 - \frac{1}{r^2}\right) \sin 2\theta \ln \frac{1 + 2r \sin \theta + r^2}{1 - 2r \sin \theta + r^2} \end{aligned} \quad (2.14)$$

for the interior flow. It can be confirmed that (2.14) does satisfy the equations plus conditions, noting, in particular, that Ψ is analytic at $r=0$. Of importance for later calculations, we see that the slip velocities on the boundary are

$$\mathcal{U}(r, -\frac{1}{2}\pi) = -\mathcal{U}(r, \frac{1}{2}\pi) = \frac{1-r^4}{2\pi r^3} \ln \frac{1+r}{1-r} - \frac{1-r^2}{\pi r^2}, \quad (2.15)$$

and

$$\mathcal{V}(1, \theta) = \cos^2 \theta - 2\pi^{-1} \cos \theta \{1 - \sin \theta \ln(\sec \theta + \tan \theta)\}. \quad (2.16)$$

These functions are graphed in Fig. 1; the velocity at the origin is clearly non-zero. The streamlines for the interior flow are simple closed contours inside the semi-circle, with a single stagnation point where $r \approx 0.4802$, $\theta = 0$; the pattern is shown in Fig. 2.

The mass flux balance will be maintained through the existence of free shear layers around the perimeter of the semi-circular region $r = 1$, $\theta = \pm \frac{1}{2}\pi$. Along $r = 1$ there will be the $\frac{1}{3}$ and

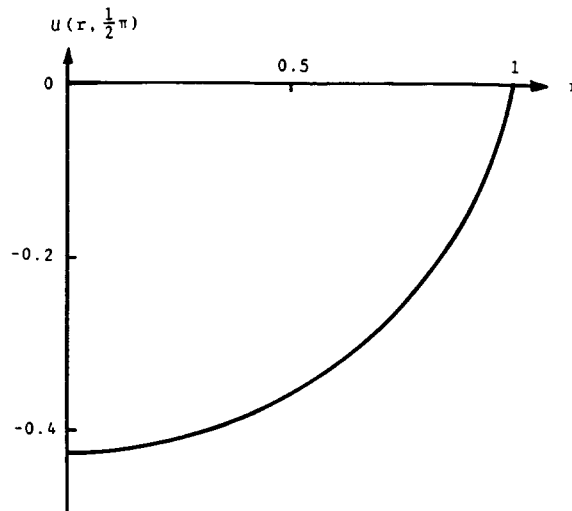


Fig. 1(a). Graph of the slip velocity $\mathcal{U}(r, \frac{1}{2}\pi)$ as given by (2.15).

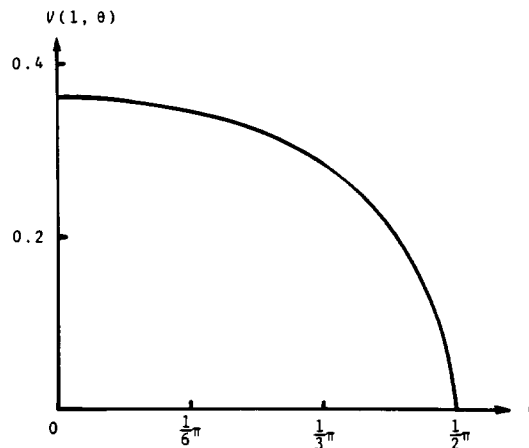


Fig. 1(b). Graph of the slip velocity $\mathcal{V}(1, \theta)$ as given by (2.16).

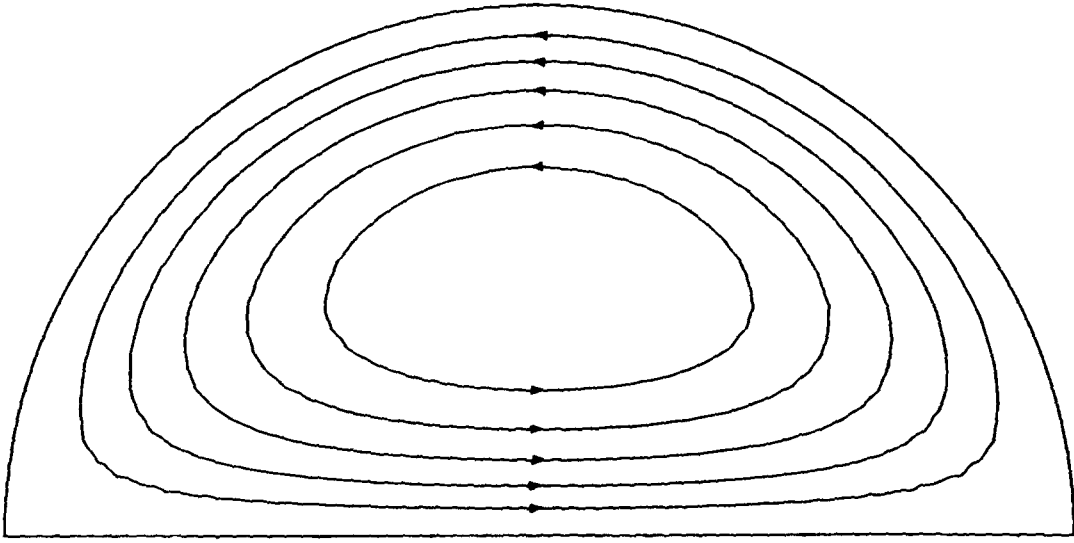


Fig. 2. Streamlines of the $O(1)$ interior flow for the values $\Psi = 0.0, 0.08, 0.14, 0.2, 0.26, 0.32$.

$\frac{1}{4}$ -layers which are fed fluid from the radially outward flow in the Ekman layer on the lower disc. The behaviour here is expected to be equivalent to the classical flow in axisymmetric Stewartson layers for the split-disc problem (cf. Stewartson [1], Moore and Saffman [2]), slightly modified by the asymmetry in the interior.

For the $\frac{1}{4}$ -layer the axial pressure gradient is zero, and so we write $r - 1 = E^{\frac{1}{4}}\sigma$, $u = E^{\frac{1}{4}}u_1(\sigma, \theta)$, $v = v_1(\sigma, \theta)$, $w = E^{\frac{1}{4}}(z - \frac{1}{2}h)w_1(\sigma, \theta)$, $p = E^{\frac{1}{4}}p_1(\sigma, \theta)$ so that the governing equations (2.1–2.4) are seen to reduce to

$$p_{1\sigma\sigma\sigma} + 4w_1 = 0 \quad \text{with} \quad v_1 = \frac{1}{2}p_{1\sigma}, \quad u_1 = -\frac{1}{2}p_{1\theta} + \frac{1}{4}p_{1\sigma\sigma}. \quad (2.17)$$

The Ekman condition on the discs show

$$2hw_1 = -p_{1\sigma\sigma}, \quad (2.18)$$

and the boundary conditions to be satisfied require $v_1 \rightarrow 0$ as $\sigma \rightarrow +\infty$ and $v_1 \sim \mathcal{V}(1, \theta)$ as $\sigma \rightarrow -\infty$ to ensure a match with the interior flow. The solution for this pair of equations which ensures that v_1 and $v_{1\sigma}$ are continuous across $\sigma = 0$, the smoothest solution possible is

$$v = \begin{cases} \frac{1}{2}\mathcal{V}(1, \theta)\{2 - e^{(2/h)^{\frac{1}{4}}\sigma}\}, & \sigma < 0 \\ \frac{1}{2}\mathcal{V}(1, \theta)e^{-(2/h)^{\frac{1}{4}}\sigma}, & \sigma > 0 \end{cases}; \quad (2.19a)$$

the radial and axial velocity components then follow, with

$$u = \begin{cases} -E^{\frac{1}{4}}\mathcal{V}_\theta(1, \theta)\left\{\sigma - \frac{1}{2}\left(\frac{h}{2}\right)^{\frac{1}{4}}e^{(2/h)^{\frac{1}{4}}\sigma}\right\}, & \sigma < 0 \\ \frac{1}{2}E^{\frac{1}{4}}\left(\frac{h}{2}\right)^{\frac{1}{4}}\mathcal{V}_\theta(1, \theta)e^{-(2/h)^{\frac{1}{4}}\sigma}, & \sigma > 0 \end{cases}; \quad (2.19b)$$

$$w = -\frac{E^{\frac{1}{4}}}{4} \left(\frac{2}{h}\right)^{\frac{1}{2}} \left(1 - \frac{2z}{h}\right) \mathcal{V}(1, \theta) e^{-(2/h)^{\frac{1}{2}}|\sigma|}. \quad (2.19c)$$

The presence of the $\frac{1}{3}$ -layer to ensure the continuity of angular stress, as well as complete the mass flux balance, is again clear, and here we introduce the notation $r-1 = E^{\frac{1}{4}}\rho$, $u = E^{\frac{1}{4}}u_0(\rho, \theta, z)$, $v = E^{\frac{1}{4}}v_0(\rho, \theta, z)$, $w = E^{\frac{1}{4}}w_0(\rho, \theta, z)$, $p = E^{\frac{1}{4}}p_0(\rho, \theta, z)$. The governing equations for asymmetric flows are the same as those given by Greenspan [3], with

$$p_{0\rho\rho\rho} + 4w_{0z} = 0, \quad w_{0\rho\rho} = p_{0z} \quad \text{and} \quad 2v_0 = p_{0\rho}, \quad (2.20)$$

which are independent of θ , though the radial velocity follows as $u_0 = -\frac{1}{2}p_{0\theta} + \frac{1}{4}p_{0\rho\rho}$. However, the solution for p_0 and w_0 which smoothens the discontinuity shown in (2.19) is no different from that given by Moore and Saffman [2], and can be written down directly as

$$w_0 + iv_0 = \frac{1}{2\pi} \mathcal{V}(1, \theta) \int_{-\infty}^{\infty} \frac{e^{-1\alpha\rho} e^{-\frac{1}{2}\alpha^3(z-h)}}{\sinh(\frac{1}{2}\alpha^3h)} d\alpha. \quad (2.21)$$

We next turn to the behaviour in the shear layer along $\theta = -\frac{1}{2}\pi$, with the expectation that a reflection of this behaviour in the origin will give the flow along $\theta = +\frac{1}{2}\pi$. There are two requirements of this region: first to ensure continuity in the radial velocity from $\mathcal{U}(r, -\frac{1}{2}\pi)$ as given by (2.15) when $\theta \rightarrow -\frac{1}{2}\pi +$, to zero when $\theta \rightarrow -\frac{1}{2}\pi -$, and second to absorb the fluid brought to the slit along $\theta = -\frac{1}{2}\pi$ within the Ekman layer on the lower disc. (Although the flow in the Ekman layer towards $r = 1$ and towards $\theta = -\frac{1}{2}\pi$ is different, the Stewartson layers just “see” the Ekman layer as a delta function, and so the difference is irrelevant except for the very small domain of magnitude $O(E^{\frac{1}{4}})$ along the split.) This understanding makes clear the analogy with the shear layer flow along $r = 1$ for both requirements, and so it is reasonable to conjecture from the beginning that there is a similar structure. Therefore, for the inner layer, we introduce the variable ω by $r(\theta + \frac{1}{2}\pi) = E^{\frac{1}{4}}\omega$, and then write the dependent variables as $u = E^{\frac{1}{4}}U_0(r, \omega, z)$, $v = E^{\frac{1}{4}}V_0(r, \omega, z)$, $w = E^{\frac{1}{4}}W_0(r, \omega, z)$, $p = E^{\frac{1}{4}}P_0(r, \omega, z)$. When these are substituted into (2.1–2.4), there follow the equations $U_{0r} + \omega r^{-1}U_{0\omega} + r^{-1}U_0 + V_{0\omega} + W_{0z} = 0$, $-2V_0 = -P_{0r} - \omega r^{-1}P_{0\omega} + U_{0\omega\omega}$, $2U_0 = -P_{0\omega}$, $0 = -P_{0z} + W_{0\omega\omega}$, respectively, and eliminating U_0 and V_0 leads to

$$P_{0\omega\omega\omega\omega} + 4W_{0z} = 0, \quad W_{0\omega\omega} = P_{0z} \quad \text{and} \quad 2V_0 = -P_{0\omega}, \quad (2.22)$$

which have exactly the same form as (2.20).

Further, for the outer layer we define $r(\theta + \frac{1}{2}\pi) = E^{\frac{1}{4}}\eta$, plus $u = U_1(r, \eta)$, $v = E^{\frac{1}{4}}V_1(r, \eta)$, $w = E^{\frac{1}{4}}(z - \frac{1}{2}h)W_1(r, \eta)$, $p = E^{\frac{1}{4}}P_1(r, \eta)$, which show

$$P_{1\eta\eta\eta\eta} + 4W_1 = 0 \quad \text{with} \quad U_1 = -\frac{1}{2}P_{1\eta}, \quad V_1 = \frac{1}{2}(P_{1r} + \eta r^{-1}P_{1\eta}),$$

equivalent to (2.17). Consequently, the solutions can be written down immediately as

$$U_1 = \begin{cases} \frac{1}{2}\mathcal{U}(r, -\frac{1}{2}\pi)\{2 - e^{(2/h)^{\frac{1}{2}}\eta}\}, & \eta < 0 \\ \frac{1}{2}\mathcal{U}(r, -\frac{1}{2}\pi)e^{-(2/h)^{\frac{1}{2}}\eta}, & \eta > 0 \end{cases} \quad (2.23)$$

with

$$w = -\frac{E^{\frac{1}{4}}}{4} \left(\frac{2}{h}\right)^{\frac{1}{2}} \left(1 - \frac{2z}{h}\right) \mathcal{U}(r, -\frac{1}{2}\pi) e^{-(2/h)^{\frac{1}{2}}|z|}.$$

Similarly, in the $\frac{1}{3}$ -layer, the corresponding form to (2.21) is

$$W_0 + iV_0 = \frac{1}{2\pi} \mathcal{U}(r, -\frac{1}{2}\pi) \int_{-\infty}^{\infty} \frac{e^{-i\alpha\omega} \cdot e^{-\frac{1}{2}\alpha^3(z-h)}}{\sinh(\frac{1}{2}\alpha^3 h)} d\alpha.$$

It is now easily seen that the flow in the layers along $\theta = +\frac{1}{2}\pi$ is given on reflection from that now given for $\theta = -\frac{1}{2}\pi$. Therefore, the structure of the behaviour in the asymmetric Stewartson layers is exactly that for the axisymmetric layers, with the only difference being in the magnitude of the velocities, which are determined directly from the slip velocities as calculated from the inviscid flow in the interior.

Here a semi-circular region has been taken as that where there is a different rotation rate, but it is clear that when the shape of the region is changed the only separate calculation required is to solve (2.12) for the new region. The slip velocity along the boundary can then be determined directly, and thereby fully determine the flow in the Stewartson layers. The solution of the Poisson equation (2.12) is a classical problem with many well known results in the literature. For example, with the elliptical region $x^2/a^2 + y^2/b^2 = 1$, it is easily seen that

$$\Psi = -\frac{a^2 b^2}{2(a^2 + b^2)} \left(\frac{x^2}{a^2} + \frac{y^2}{b^2} - 1\right);$$

the streamlines are also ellipses, which are similar to the boundary.

3. The effect of a solid sidewall

As a variation to the previous problem, we now consider the same semi-circular domain as before, i.e. $r \leq 1$, $|\theta| \leq \frac{1}{2}\pi$, between two differentially rotating discs – see the conditions (2.5) – except that now it is enclosed by a solid sidewall along $r = 1$, $|\theta| = \frac{1}{2}\pi$. The Stewartson $\frac{1}{4}$ and $\frac{1}{3}$ -layers present at the sidewall play a role in completing the mass flux balance as before, but instead of establishing the continuity of velocities and shear stresses, the layers now have to satisfy no-slip conditions, which are written as

$$u = v = w = 0 \quad \begin{array}{l} \text{for } r = 1, \quad |\theta| < \frac{1}{2}\pi, \\ \text{and } \theta = \pm \frac{1}{2}\pi, \quad 0 < r < 1. \end{array} \quad (3.1)$$

This particular problem has been addressed by van Heijst [7], and here we will merely summarize the main results presented in that study.

To leading order, the geostrophic interior flow will not be affected by the presence of the sidewall, so the flow in this configuration is also described by (2.14). It can be shown by standard analysis that the leading-order azimuthal, axial and radial velocity components in the $\frac{1}{4}$ -layer along $r = 1$ are

$$v = \mathcal{V}(1, \theta) \{1 - e^{(2/h)^{\frac{1}{2}}\sigma}\}, \quad (3.2a)$$

$$w = -\frac{1}{2} E^{\frac{1}{2}} \left(\frac{2}{h}\right)^{\frac{1}{2}} \left(1 - \frac{2z}{h}\right) \mathcal{V}(1, \theta) e^{(2/h)^{\frac{1}{2}} \sigma}, \quad (3.2b)$$

$$u = -E^{\frac{1}{2}} \mathcal{V}_\theta(1, \theta) \left[\sigma + \left(\frac{h}{2}\right)^{\frac{1}{2}} \{1 - e^{(2/h)^{\frac{1}{2}} \sigma}\} \right], \quad (3.2c)$$

$\mathcal{V}(1, \theta)$ is given by (2.16).

In the $\frac{1}{3}$ -layer, the leading-order velocity field $(u, v, w) = (E^{\frac{1}{2}}U_0, E^{\frac{1}{2}}V_0, E^{\frac{1}{2}}W_0)$ has to complete the vertical $O(E^{\frac{1}{2}})$ flux balance, and the solutions for V_0 and W_0 are

$$(V_0, W_0) = -\frac{4}{\sqrt{3}h} \sum_{n=1}^{\infty} \gamma_n^{-2} \Phi_n(\rho) \left(\cos \frac{n\pi z}{h}, \sin \frac{n\pi z}{h} \right), \quad (3.3)$$

where $\Phi_n(\rho) = e^{\frac{1}{2}\gamma_n \rho} \sin(\frac{1}{2}\sqrt{3}\gamma_n \rho)$ and $\gamma_n = (2n\pi/h)^{\frac{1}{2}}$. In contrast to the solution (2.21) for the detached layer (which had to ensure the continuity of lateral stress), this solution is independent of θ . However, the higher-order fields, for example $(u, v, w) = (E^{\frac{1}{2}}\tilde{U}_0, E^{\frac{1}{2}}\tilde{V}_0, E^{\frac{1}{2}}\tilde{W}_0)$, required for satisfying the no-slip conditions of higher-order velocities in the $\frac{1}{4}$ -layer, do exhibit a dependence on θ .

Now we will examine the matching of this Stewartson layer along $r = 1$ to the geostrophic interior. Generally, the interior flow variables are expanded in powers of $E^{\frac{1}{4}}$ (cf. Johnson [5] and van Heijst [7]) as

$$(\mathcal{U}, \mathcal{V}) = \sum_{j=0}^{\infty} (\mathcal{U}^{(j)}, \mathcal{V}^{(j)}) E^{j/4} \quad (3.4)$$

where just the $j = 0$ terms have been found so far. Each term is then written as a Taylor series expansion for $r \rightarrow 1$, and, using $r - 1 = E^{\frac{1}{2}}\sigma$, one finds for the radial components, that

$$\lim_{r \rightarrow 1} \mathcal{U}^{(j)} = \mathcal{U}^{(j)}(1, \theta) + E^{\frac{1}{2}} \sigma \mathcal{U}_r^{(j)}(1, \theta) + \frac{1}{2} E^{\frac{1}{2}} \sigma^2 \mathcal{U}_{rr}^{(j)}(1, \theta) + O(E^{\frac{3}{4}}), \quad (3.5)$$

and so

$$\begin{aligned} \lim_{r \rightarrow 1} \mathcal{U} &= U^{(0)}(1, \theta) + E^{\frac{1}{4}} \{ \sigma \mathcal{U}_r^{(0)}(1, \theta) + \mathcal{U}^{(1)}(1, \theta) \} \\ &+ E^{\frac{1}{2}} \{ \frac{1}{2} \sigma^2 \mathcal{U}_{rr}^{(0)}(1, \theta) + \sigma \mathcal{U}_r^{(1)}(1, \theta) + \mathcal{U}^{(2)}(1, \theta) \} + O(E^{\frac{3}{4}}). \end{aligned} \quad (3.6)$$

There is a corresponding expression for $\lim_{r \rightarrow 1} \mathcal{V}$.

In the $\frac{1}{4}$ -layer the radial velocity is expanded as

$$u(\sigma, \theta) = E^{\frac{1}{4}} u_1(\sigma, \theta) + E^{\frac{1}{2}} u_2(\sigma, \theta) + O(E^{\frac{3}{4}}). \quad (3.7)$$

For the present analysis it suffices to consider only the $O(E^{\frac{1}{4}})$ terms, and with (3.2c) one obtains

$$u \sim -E^{\frac{1}{4}} \left\{ \sigma + \left(\frac{h}{2}\right)^{\frac{1}{2}} \right\} \mathcal{V}_\theta^{(0)}(1, \theta) + O(E^{\frac{1}{2}}) \quad \text{as } \sigma \rightarrow -\infty. \quad (3.8)$$

This solution should match with the interior solution for $\lim_{r \rightarrow 1} \mathcal{U}$ as given by (3.6), and, since $\mathcal{U}^{(0)}(1, \theta) = 0$, this requires

$$U_r^{(0)}(1, \theta) = -\mathcal{V}_\theta^{(0)}(1, \theta), \quad (3.9a)$$

$$U^{(1)}(1, \theta) = -\left(\frac{h}{2}\right)^{\frac{1}{2}} \mathcal{V}_\theta^{(0)}(1, \theta). \quad (3.9b)$$

Although (3.9a) is identical to the continuity equation of the $O(1)$ interior flow evaluated at $r = 1$, (3.9b) acts as a boundary condition for the $O(E^{\frac{1}{2}})$ interior flow. This is an important result, which reflects the influence of the sidewall upon the geostrophic flow in the interior domain. If one would carry out the same matching technique for the detached $\frac{1}{4}$ -layer (Section 2) (i.e. by substituting (2.19b) into (3.7) and matching with (3.6)) this would result in $\mathcal{U}^{(1)}(1, \theta) = 0$, implying that no higher-order interior flow is induced in that case.

A comparison between Stewartson's original (axisymmetric) split-disc problem, the asymmetric split-disc problem as discussed in the previous section, and the present problem, then leads to the (general) conclusion that the $\frac{1}{4}$ -layer induces higher-order interior flow provided that (i) the layer is *asymmetric* (i.e. shows dependence on its lateral co-ordinate) and (ii) the layer is *attached* to a solid wall.

The attached Stewartson layer along $|\theta| = \frac{1}{2}\pi$ also shows a dependence on its lateral co-ordinate, and so similar effects can be expected here as well. For the moment we concentrate on the layer along $\theta = -\frac{1}{2}\pi$, where the leading-order velocities in the $\frac{1}{4}$ -layer (using the same notation as that in Section 2) are found to be

$$u = \mathcal{U}^{(0)}(r, -\frac{1}{2}\pi) \{1 - e^{-(2/h)^{\frac{1}{2}}\eta}\}, \quad (3.10a)$$

$$w = -\frac{1}{2} E^{\frac{1}{2}} \left(\frac{2}{h}\right)^{\frac{1}{2}} \left(1 - \frac{2z}{h}\right) \mathcal{U}^{(0)}(r, -\frac{1}{2}\pi) e^{-(2/h)^{\frac{1}{2}}\eta}, \quad (3.10b)$$

$$v = -E^{\frac{1}{2}} \mathcal{U}_r^{(0)}(r, -\frac{1}{2}\pi) \left[\eta - \left(\frac{h}{2}\right)^{\frac{1}{2}} \{1 - e^{-(2/h)^{\frac{1}{2}}\eta}\} \right]; \quad (3.10c)$$

where $r(\theta + \frac{1}{2}\pi) = E^{\frac{1}{2}}\eta$ here.

In the $\frac{1}{3}$ -layer, the principal velocity field $(u, w) = E^{\frac{1}{2}}(U_0, W_0)$ has to complete the vertical $O(E^{\frac{1}{2}})$ flux balance, and the solutions can be found by standard techniques as

$$(U_0, W_0) = -\frac{4r}{\sqrt{3}h} \sum_{n=1}^{\infty} \gamma_n^{-2} \Phi_n(\omega) \left(\cos \frac{n\pi z}{h}, \sin \frac{n\pi z}{h} \right) \quad (3.11)$$

with γ_n and Φ_n given by (3.3), plus $r(\theta + \frac{1}{2}\pi) = E^{\frac{1}{2}}\omega$. Higher-order fields (i.e. smaller than $O(E^{\frac{1}{2}})$) play a role in matching higher-order $\frac{1}{4}$ -layer velocities to the solid wall, but details of this analysis are not presented here. It is obvious that the solutions of the $\frac{1}{4}$ and $\frac{1}{3}$ -layers along $\theta = +\frac{1}{2}\pi$ are derived by reflection.

We next turn to the matching of the solution in the $\frac{1}{4}$ -layer along $\theta = -\frac{1}{2}\pi$ to that in the interior. For this purpose, it is convenient to introduce the angle $\phi = \theta + \frac{1}{2}\pi$, so that the wall now occupies $\phi = 0$. Consequently,

$$E^{\frac{1}{2}}\eta = r\phi + O(\phi^3) \quad \text{as } \phi \rightarrow 0, \quad (3.12)$$

(see Fig. 3). Further, we decompose the interior velocity $(\mathcal{U}, \mathcal{V})$ into components $(\mathcal{U}^*, \mathcal{V}^*)$ parallel and perpendicular to the wall, respectively, with

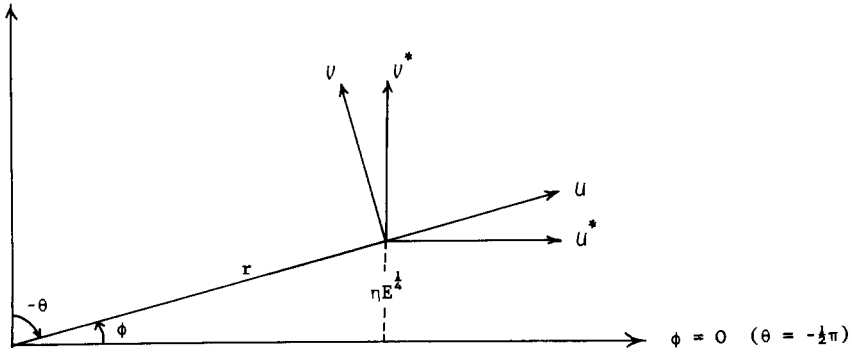


Fig. 3. Diagram illustrating the geometrical relationship between (u, v) and (u^*, v^*) .

$$u^* = u \cos \phi - v \sin \phi, \quad v^* = u \sin \phi + v \cos \phi.$$

It then follows that

$$\begin{aligned} \lim_{\phi \rightarrow 0} u^* &= u(r, -\tfrac{1}{2}\pi) + \phi \{u_\theta(r, -\tfrac{1}{2}\pi) - v(r, -\tfrac{1}{2}\pi)\} + \tfrac{1}{2}\phi^2 \{u_{\theta\theta}(r, -\tfrac{1}{2}\pi) \\ &\quad - u(r, -\tfrac{1}{2}\pi) - 2v_\theta(r, -\tfrac{1}{2}\pi)\} + \dots \end{aligned} \quad (3.13)$$

As before, $u^* = \sum_{j=0}^{\infty} E^{j/4} u^{*(j)}$, and by using (3.12) and (3.13) one derives

$$\begin{aligned} \lim_{\phi \rightarrow 0} u^* &= u^{(0)}(r, -\tfrac{1}{2}\pi) + E^{\frac{1}{4}} [r^{-1} \eta \{u_\theta^{(0)}(r, -\tfrac{1}{2}\pi) - v^{(0)}(r, -\tfrac{1}{2}\pi)\} \\ &\quad + u^{(1)}(r, -\tfrac{1}{2}\pi)] + O(E^{\frac{1}{2}}) \end{aligned} \quad (3.14a)$$

and, likewise,

$$\begin{aligned} \lim_{\phi \rightarrow 0} v^* &= v^{(0)}(r, -\tfrac{1}{2}\pi) + E^{\frac{1}{4}} [r^{-1} \eta \{v_\theta^{(0)}(r, -\tfrac{1}{2}\pi) + u^{(0)}(r, -\tfrac{1}{2}\pi)\} \\ &\quad + v^{(1)}(r, -\tfrac{1}{2}\pi)] + O(E^{\frac{1}{2}}). \end{aligned} \quad (3.14b)$$

These expressions must be matched to the composite $\frac{1}{4}$ -layer solutions (3.10) of the corresponding order:

$$\lim_{\eta \rightarrow \infty} u = u^{(0)}(r, -\tfrac{1}{2}\pi) + O(E^{\frac{1}{4}}), \quad (3.15a)$$

$$\lim_{\eta \rightarrow \infty} v = -\left\{ \eta - \left(\frac{h}{2}\right)^{\frac{1}{2}} \right\} E^{\frac{1}{4}} u_r^{(0)}(r, -\tfrac{1}{2}\pi) + O(E^{\frac{1}{2}}), \quad (3.15b)$$

which require

$$v_\theta^{(0)}(r, -\tfrac{1}{2}\pi) + u^{(0)}(r, -\tfrac{1}{2}\pi) + r u_r^{(0)}(r, -\tfrac{1}{2}\pi) = 0, \quad (3.16a)$$

$$v^{(1)}(r, -\tfrac{1}{2}\pi) = \left(\frac{h}{2}\right)^{\frac{1}{2}} u_r^{(0)}(r, -\tfrac{1}{2}\pi). \quad (3.16b)$$

The first result (3.16a) is identical to the continuity equation for the interior flow evaluated along $\theta = -\frac{1}{2}\pi$, but the second requirement (3.16b) provides a boundary condition for the $O(E^{\frac{1}{4}})$ interior flow. As with the matching for the $\frac{1}{4}$ -layer along $r = 1$, it is found here that the Stewartson $\frac{1}{4}$ -layer induces a higher-order interior flow, in the sense that it provides a condition for the higher-order velocity normal to the layer. It is easily checked that completing the matching along the wall at $\theta = +\frac{1}{2}\pi$ requires

$$\mathcal{V}^{(1)}(r, \frac{1}{2}\pi) = \left(\frac{h}{2}\right)^{\frac{1}{2}} \mathcal{U}_r^{(0)}(r, -\frac{1}{2}\pi). \quad (3.17)$$

Therefore, we can now determine the $O(E^{\frac{1}{4}})$ interior circulation. The stream function Ψ for the interior flow is given by the expansion $\Psi = \sum_{j=0}^{\infty} E^{j/4} \Psi^{(j)}(r, \theta)$, where $\Psi^{(0)}$ is given by (2.14). For the $O(E^{\frac{1}{4}})$ flow, it can be shown (as was done for the $O(1)$ flow in Section 2) that

$$\nabla^2 \Psi^{(1)} = 0 \quad (3.18)$$

with $\mathcal{U}^{(1)} = r^{-1} \Psi_{\theta}^{(1)}$, $\mathcal{V}^{(1)} = -\Psi_r^{(1)}$. This Laplace equation is to be solved subject to the boundary conditions (3.9b), (3.16b) and (3.17), which become

$$\Psi^{(1)} = -\left(\frac{h}{2}\right)^{\frac{1}{2}} \mathcal{V}^{(0)}(1, \theta) \quad \text{on } r = 1, |\theta| < \frac{1}{2}\pi, \quad (3.19)$$

$$\Psi^{(1)} = -\left(\frac{h}{2}\right) \mathcal{U}^{(0)}(r, -\frac{1}{2}\pi) \quad \text{on } |\theta| = \frac{1}{2}\pi, 0 < r < 1,$$

where the integration constants have been taken as zero to ensure continuity of $\Psi^{(1)}$ in the corners of the domain. The solution of (3.18), subject to (3.19), is obtained in terms of the Fourier series

$$\begin{aligned} \Psi^{(1)}(r, \theta) = & A \sum_{n=0}^{\infty} (-1)^n b_n r^{2n} \cos 2n\theta - A \sum_{n=0}^{\infty} (-1)^n c_n r^{2n+1} \sin(2n+1)\theta \\ & + 2A\pi^{-1} \sum_{n=0}^{\infty} \sum_{m=1}^{\infty} \alpha_{nm} b_n r^m \sin m(\theta + \frac{1}{2}\pi), \end{aligned} \quad (3.20)$$

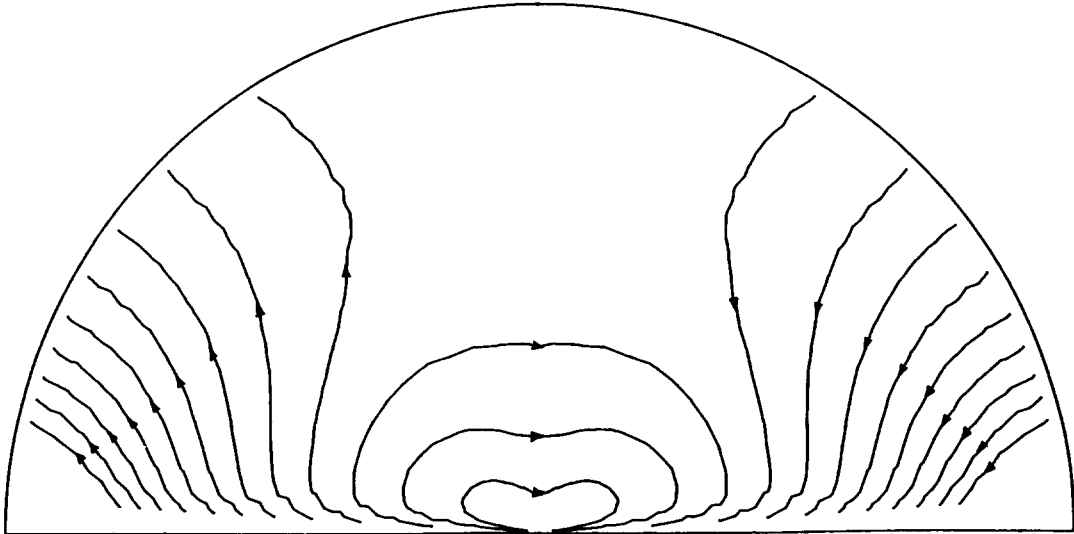


Fig. 4. Streamlines of the $O(E^{\frac{1}{4}})$ interior flow for the values $\Psi^{(1)} = -0.6, -0.65, -0.7, \dots, -1.15$.

where $A = 4\pi^{-1}(\frac{1}{2}h)^{\frac{1}{2}}$, $b_n = \{(2n-1)(2n+3)\}^{-1}$, $c_n = \{(2n+1)(2n+3)\}^{-1}$, $\alpha_{nm} = m\{1 - (-1)^m\}(4n^2 - m^2)^{-1}$ (see van Heijst [7]). It is not possible to sum the third series in terms of elementary functions. Figure 4 represents the streamline pattern for the $O(E^{\frac{1}{4}})$ circulation calculated from (3.20). This $O(E^{\frac{1}{4}})$ flow pattern should be superimposed on the $O(1)$ pattern shown in Figure 2, though clearly the difference is slight when E is very small, as in most cases of interest.

4. Discussion and conclusions

In this paper we have addressed two different asymmetric geometries in which Stewartson layers occur: one in which the Stewartson layer is detached (Section 2), and one in which it is attached to a solid vertical wall (Section 3). It was shown for the detached case that the asymmetry does not lead to any drastic changes on the layer structure, and the solutions are very similar to those obtained for axisymmetric problems. The axisymmetric Stewartson layer plays a rather *passive* role on providing a specified vertical $O(E^{\frac{1}{4}})$ flux and in establishing a smooth matching between two geostrophically-controlled flow regions. The structure of the asymmetric Stewartson layer and the flow outside it become essentially more complicated when the layer is attached to a solid wall: it was shown in Section 3 by a matching analysis that (besides contributing to the flux balance and establishing a matching of the $O(1)$ interior flow to the boundary) the asymmetric layer induces higher-order flow in the geostrophic interior region. In this sense the asymmetric attached Stewartson layer plays an *active* part in the flow system.

The analysis presented in Section 3 was only carried out to $O(E^{\frac{1}{4}})$, but an extended analysis to higher orders reveals the existence of a complicated mutual interaction between the geostrophic interior and the Stewartson $\frac{1}{4}$ and $\frac{1}{3}$ -layers at the wall (see van Heijst [7]). For the general case of an asymmetric Stewartson layer attached to a solid boundary, the structure of this interaction is shown schematically in Fig. 5. The various flow variables in the interior, the $\frac{1}{4}$ -layer and the $\frac{1}{3}$ -layer are expanded in powers of $E^{\frac{1}{4}}$, $E^{\frac{1}{4}}$ and $E^{\frac{1}{12}}$, respectively, and the following notation is used:

$$\begin{aligned} \text{interior: } (u, v, w) &= \sum_{j=0}^{\infty} (Q^{(j)}, \mathcal{V}^{(j)}, E^{\frac{1}{4}}\mathcal{W}^{(j)})E^{j/4}, \\ \frac{1}{4}\text{-layer: } (u, v, w) &= \sum_{j=0}^{\infty} (E^{\frac{1}{4}}\bar{u}^{(j)}, \bar{v}^{(j)}, E^{\frac{1}{4}}\bar{w}^{(j)})E^{j/4}, \\ \frac{1}{3}\text{-layer: } (u, v, w) &= \sum_{m=0}^{\infty} (E^{\frac{1}{12}}\tilde{u}^{(m)}, \tilde{v}^{(m)}, \tilde{w}^{(m)})E^{m/12}, \end{aligned}$$

with u and v being the velocity components (expressed in some locally orthogonal coordinate system) perpendicular to and tangential to the boundary, respectively, and w being the vertical velocity component. As can be seen in Fig. 5, the matching of the interior flow of $O(E^{j/4})$ requires a velocity $\bar{v}^{(j)}$ of $O(E^{j/4})$, and the normal velocity component $\bar{u}^{(j)}$ of $O(E^{(j+1)/4})$ associated with $\bar{v}^{(j)}$ induces – in turn – interior flow of $O(E^{(j+1)/4})$, and so on. The vertical $\frac{1}{4}$ -layer velocity $\bar{w}^{(j)}$ is matched to the wall (no-slip condition) by the $\frac{1}{3}$ -layer, which also provides a condition for the next-order $\bar{v}^{(j+1)}$ at $\sigma=0$. In the $\frac{1}{4}$ -layer $\bar{w}^{(j)}$ contributes to a vertical flux of $O(E^{(j+2)/4})$, which generally does not balance the Ekman

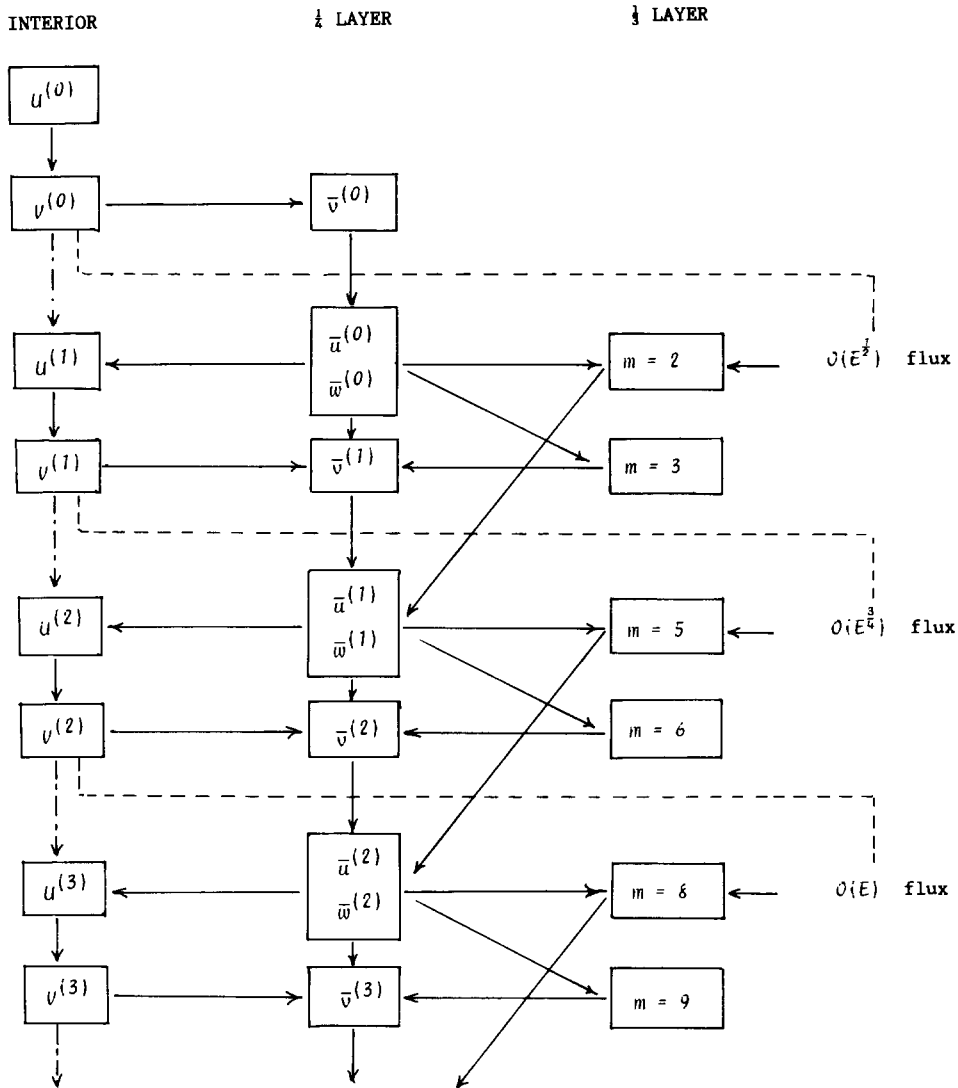


Fig. 5. Diagram illustrating the interaction between the interior region and the attached Stewartson $\frac{1}{4}$ and $\frac{1}{3}$ -layers in an asymmetric configuration.

transports of this order, and an additional contribution of $O(E^{(j+2)/4})$ by the $\frac{1}{3}$ -layer is required. This is accomplished by the field $m = 3j + 2$, which in turn provides a condition for $\bar{u}^{(j+1)}$ at $\sigma = 0$. Due to the action of the Ekman layers present at the horizontal boundaries, the horizontal $O(E^{j/4})$ interior flow drives a vertical flux of $O(E^{(j+2)/4})$, which implies an indirect interaction with the $\frac{1}{3}$ -layer (in Fig. 5 indicated by dashed lines). It is obvious that in the absence of any higher-order interior flow (as in axisymmetric problems) the interaction structure reduces to a much more simple form.

To conclude, we note that the formation of free shear layers for axisymmetric flows has recently been investigated by Smith [8], and it is now seen that these results can be extended to situations where asymmetries are present. Taking the geometry of the semicircular disc, we consider the situation where this disc is given its extra angular velocity impulsively at time

$t = 0$. Formally, the Ekman layers form during the time $t = O(1)$, though practically they are complete after a few revolutions.

Smith [8] showed that it is during the period where $1 \ll t \ll E^{-\frac{1}{3}}$ that geostrophic forces lead to a concentration of the flow in a vertical layer with width $O(t^{-1})$; we see that the asymmetry does not alter this conclusion. For example, for the layer along $r = 1$, $|\theta| < \frac{1}{2}\pi$, we write $\lambda = (r - 1)t = O(1)$ and $w = (r - 1)^{-1}\bar{w}(\lambda, \theta, z)$ for

$$\lambda^2 \bar{w}_{\lambda\lambda\lambda\lambda} + 2\lambda \bar{w}_{\lambda\lambda\lambda} + 4\bar{w}_{zz} = 0, \quad (4.1)$$

which is independent of θ . The remaining quantities follow with $u = \bar{u}(\lambda, \theta, z)$, $v = (r - 1)^{-1}\bar{v}(\lambda, \theta, z)$ and $p = \bar{p}(\lambda, \theta, z)$ through $2\bar{v} = \lambda\bar{p}$, $\bar{p}_z = -\bar{w}_\lambda$, $2\bar{u} = -\bar{p}_\theta - \bar{v}_\lambda$. The variable θ only enters the solution for \bar{w} , \bar{v} and \bar{p} as the coefficient of the solution to (4.1) as given by axisymmetric theory; the actual value of the coefficient follows from the mass flux requirement that the quantity of fluid flowing vertically within the layer must be equal to that brought to $r = 1$ through the Ekman layer for each value of θ .

Next, when we consider the behaviour in the layer along $\theta = -\frac{1}{2}\pi$, $r < 1$, we can write $\mu = r(\theta + \frac{1}{2}\pi)t$ and $w = r^{-1}(\theta + \frac{1}{2}\pi)^{-1}\bar{W}(r, \mu, z)$ for

$$\mu^2 \bar{W}_{\mu\mu\mu\mu} + 2\mu \bar{W}_{\mu\mu\mu} + 4\bar{W}_{zz} = 0,$$

exactly the same as (4.1). The formation of the layer along $\theta = -\frac{1}{2}\pi$ is given by the same process as that along $r = 1$, and the analytical solution requires only an adjustment to the coefficient.

It is now no more difficult to extend this discussion to the later times $t = O(E^{-\frac{1}{3}})$ when the $\frac{1}{3}$ -layer is developed, and also during the spin-up time $t = O(E^{-\frac{1}{2}})$; the same conclusions follow.

Acknowledgement

The second author wishes to thank the Natural Sciences and Engineering Research Council of Canada for a grant in aid of research during the time this work was completed.

References

1. K. Stewartson, On almost rigid rotations, *J. Fluid Mech.* 3 (1957) 17–26.
2. D.W. Moore and P.G. Saffman, The structure of free vertical shear layers in a rotating fluid and the motion produced by a slowly rising body, *Phil. Trans. Roy. Soc. A*264 (1969) 597–634.
3. H.P. Greenspan, *The Theory of Rotating Fluids*, Cambridge University Press, Cambridge (1968).
4. R. Hide, On source-sink flows in a rotating fluid, *J. Fluid Mech.* 32 (1968) 737–764.
5. J.A. Johnson, A source-sink flow in a rotating fluid, *Proc. Camb. Phil. Soc.* 75 (1974) 269–282.
6. S.J. Jacobs, The Taylor column problem, *J. Fluid Mech.* 20 (1964) 581–591.
7. G.J.F. van Heijst, On the flow in a rotating cylinder with bottom topography, Ph.D. thesis, Twente University, The Netherlands (1981).
8. S.H. Smith, The formation of Stewartson layers in a rotating fluid, *Q.J. Mech. Appl. Math.* 40 (1987) 575–594.